Heliyon 10 (2024) e36225

Contents lists available at ScienceDirect

Heliyon

journal homepage: www.cell.com/heliyon

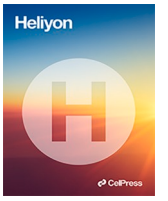

Research article

# Thermosensitive and pH-responsive quercus infectoria gall-containing gel with long-lasting anti-inflammatory activity for ulcerative colitis

Jiaojiao Bai [a], Yan Ding [a], Mubarak Iminjan [a,b,*], Kudelaidi Kuerban [a,b,*]

[a] College of Pharmacy, Xinjiang Medical University, Urumqi, 830017, China
[b] The Xinjiang Key Laboratory of Active Components and Drug Release Technology of Natural Drugs, College of Pharmacy, Xinjiang Medical University, Urumqi, Xinjiang, 830017, China

ARTICLE INFO

*Keywords:*
Quercus infectoria gall
pH/ thermosensitive gel
Ulcerative colitis
Anti-inflammatory

ABSTRACT

In the study, quercus infectoria gall (QIG) was used to develop a pH/thermosensitive gel in situ delivery system for enema administration of to treat acute ulcerative colitis (UC). The QIG ethanol extract pH/temperature-sensitive gel (QIG-pH-TSG) was characterized by using DSC, SEM, rheological and drug release analyses. The therapeutic effect in UC mice of the obtained gel were studied. The gel was maintained in a flowing liquid state under nonphysiological conditions (25 °C) to facilitate drug administration, and was transformed into a pseudoplastic liquid state under physiological conditions (37 °C), which prolonged its retention time in the colon. The gel drug was completely released within 24 h, and the temperature and viscosity of the gel were within the required range. In the *in vitro* anti-inflammatory test, QIG-pH-TSG decreased the level of TNF-α and IL-6, and increased IL-10 in RAW 264.7 actived by LPS. Moreover, the administration of QIG-pH-TSG resulted in a decrease in the colon histopathological score and an increase in colonic length, and also could reduce the IL-6, TNF-α, and C-reactive protein (CRP) levels in UC mice along with significant increases in IL-10 level in the colon. The QIG-pH-TSG could increase the concentration of QIG at the local inflammatory site and lead to an effective repair of the colonic mucosa. Therefore, the pH/thermosensitive in situ gel may serve as a drug delivery system for QIG to treat UC and overcome the limitations of some existing formulations. These results indicated that this composite gel was effectively in UC mice and the study provided a practical reference for the application of QIG-pH-TSG in the treatment of UC.

## 1. Introduction

Ulcerative colitis (UC) is a persistent and recurrent inflammatory bowel disorder that manifests primarily in the colorectal region, characterized by symptoms such as abdominal pain, diarrhea, rectal bleeding, fatigue, and unintended weight loss [1]. In recent years, there has been a notable increase in the incidence of UC, which has been attributed to improvements in living conditions and environmental factors undergoing transformation [2]. This phenomenon not only impairs the quality of life for patients but also elevates the risk of developing colorectal cancer [3]. UC's pathogenesis involves an abnormal immune response to external triggers, along with genetic, dietary, infectious, geographic and environmental factors [4]. Currently, the primary treatment modalities for UC include

* Corresponding authors. College of Pharmacy, Xinjiang Medical University, Urumqi, 830017, China.
*E-mail addresses:* 896612093@qq.com (M. Iminjan), kudelaidi@fudan.edu.cn (K. Kuerban).

https://doi.org/10.1016/j.heliyon.2024.e36225
Received 10 May 2024; Received in revised form 11 August 2024; Accepted 12 August 2024
Available online 13 August 2024

surgery, biological agents, and traditional Chinese medicine (TCM) [5]. There are positive signs that TCM can ameliorate symptoms, maintain intestinal equilibrium, facilitate intestinal mucosal repair, which is more preferable for patients with UC [6,7]. CM theory [8,9] that the progression of symptoms associated with UC, including "dysentery", "diarrhea", and "large intestinal discharge", is marked by the presence of "dampness, heat, deficiency, stasis, and toxicity". Traditional formulae such as Wu-Mei-Pill, Shenling Baizhu Powder, Huangqin Decoction, and Huangkui Lianyang Decoction have been documented to mitigate the activity of inflammatory cytokines, consequently limiting the harm inflicted on intestinal epithelial cells, which is analogous to the "dampness" aspect observed in the progression of UC [10]. Some natural compounds, for example α-Terpineol, possess various pharmacological properties that has strong protective effects against DSS-induced colitis by mitigating inflammatory and apoptotic responses [11].

Quercus infectoria gall (QIG) is the larva of Cynips gallae-tinctorice Oliv and belongs to Uyghur medicine, has been extensively utilized in clinical settings for the treatment of ulcerative colitis (UC), renowned for its potent anti-inflammatory, anti-diarrheal, and ulcer-healing properties, as reported in Refs. [12,13]. Research has demonstrated that gallnut aqueous extract has a certain therapeutic effect in reducing the inflammation in UC rats [14]. However, the conventional administration of QIG extract suspension via enema presents challenges such as high dosage, inconvenient application, short retention time, and inadequate local absorption.

Gel preparations offer direct lesion access, minimal mucosal irritation, rapid drug release, prolonged retention time, high bioavailability, avoidance of hepatic first-pass effects, and enhanced drug utilization, making them increasingly favored among localized treatment patients [15,16]. Considering the clinical features, nowadays, inflammatory bowel disease including UC can be treated with many advanced delivery technologies [17,18]. Accounting for the temperature and pH conditions at the target site (colon), the development of QIG-pH-TSG for UC treatment is tailored to respond to ambient temperature fluctuations and pH variations to induce a corresponding phase change [19,20]. This design ensures solely controlled release of QIG at the colonic site, enhancing drug efficacy with fewer side effects compared to standard oral formulations and improving patient compliance over traditional enema solutions [21].

Our team augmented and refined the QIG-pH-TSG preparation process in prior studies. In the current study, the development and physicochemical characterization of QIG-pH-TSGs, including drug release experiments, micromorphology, rheological properties, thermodynamic analysis, and sol dynamics were carried out in the first part of this study. In the latter stage of this research endeavor, the primary emphasis shifted towards evaluating the anticipated therapeutic efficacy of the developed QIG-pH-TSG formulation. Specifically, this involved a thorough analysis of its effect on dextran sulfate sodium (DSS)-induced ulcerative colitis (UC) in mice, with the ultimate goal of gaining a deeper understanding of the fundamental mechanisms underpinning the action of QIG and its derivative formulations.

## 2. Materials and methods

### 2.1. Materials

Gallic acid (purity ≥98 %), Porloxam 407, Porloxam 188 and sodium alginate were purchased from Solebao Technology (Beijing, China). Hydroxy propyl methylcellulose was purchased from Shanghai McLean Biochemistry and Science (Shanghai, China). The Sodium Dextran Sulfate (DSS) was purchased from Dalian Meilun Biotechnology (Dalian, China). Urine and faecal occult blood kit were purchased from Shanghai Yi Sheng Bio-technology (Shanghai, China). The IL-6, IL-10, TNF-α, CRP kits were purchased from Shanghai Enzymatic Biologicals (Shanghai, China). The Mesalazine enteric coated tablets was acquired from Sunflower Pharmaceutical Group Jiamusi Luling Pharmaceutical (Xinjiang, China).

### 2.2. Preparation of ethanolic extract of QIG suspension

QIG (200 g) was ground to 100 mesh powder and soaked in 60 % ethanol in a 2 L round-bottomed for 2 h, repeated three times. After filtration, the ethanol supernatant was concentrated with a vacuum rotary evaporator. Subsequently, 2 g of QIG ethanol extract was incorporated into 50 mL of water, and the resulting mixture was subjected to sonication for a duration of 30 mis, at ambient temperature conditions. This process yielded a suspension of QIG ethanol extract with a concentration of 40 mg/mL.

### 2.3. Preparation of QIG-pH-TSG gel

Poroxam 407 (P407), Poroxam 188 (P188), sodium alginate (SA) and hydroxy propyl methyl cellulose (HPMC) were used to prepare QIG-pH-TSG Gel using the cold method. Briefly, P407, P188, SA and HPMC were gradually added to distilled water under magnetic stirring in an ice bath, stirred thoroughly for about 3 min, and then the mixture was placed at 4 °C for 24 h to fully dissolve, forming a blank gel solution (referred to as blank gel). For the QIG-pH-TSG gel preparation, 1, 2 and 4 g of QIG ethanol extract were ultrasonicated with 50 mL of distilled water until completely dissolved. The resulting QIG solution (20, 40 and 80 mg/mL) were then mixed with P407, P188, SA and HPMC to form the QIG-pH-TSG gel.

### 2.4. High-performance liquid chromatography (HPLC)

The gallic acid content in the gel samples was quantified using an UltiMate 3000 HPLC system (Thermo Fisher, Waltham, MA, USA), equipped with a UV–visible detector. The chromatographic separation process employed an Agilent C18 analytical column (4.6 × 250 mm, 5 μm, California, USA), which was maintained at a temperature of 30 °C. For detection, a wavelength of 258 nm was

utilized. The mobile phase consisted of a 0.05 mM $KH_2PO_4$ solution and methanol in a volume ratio of 90:10 (v/v) flowing at a rate of 1.0 mL/min. Each sample was injected in a volume of 10 μL and subjected to a runtime of 9.0 min.

### 2.5. Physicochemical characterization of the composite gels

#### 2.5.1. The in vitro drug release test

The modified Franz diffusion cell technique [22] was employed to evaluate the drug release behavior of QIG-pH-TSG gel *in vitro*, specifically in gastric, intestinal, and colon fluids. Briefly, a mixture consisting of 15 mL of artificial gastric fluid (at a pH of 1.2), intestinal fluid (at a pH of 6.8), and colon fluid (at a pH of 7.8) was introduced into the recipient cell, while maintaining a constant temperature of 37 °C throughout the experiment. A dialysis bag soaked in release medium for 30 min was fixed between the supply cell and the receiving cell. The temperature was set at 37 °C, the speed was 600 r/min, and excess air bubbles were excluded. Stirring began after adding 1 mL of each gel to the supply cell. The entire receiver solution was removed at 0.5, 1, 2, 4, 6, 8, 10, 12, and 24 h and was immediately supplemented with blank receiver solution at the same temperature. A 0.22 μm microporous filter membrane was employed to filter the release solution. The assays were conducted in accordance with chromatographic standards, wherein peak areas were meticulously recorded. The overall drug release percentage was subsequently computed using the flow equations (I) and (II):

$$Q_n = C_n \times V_n + \sum_{i=1}^{n-1} C_i \times V_i \quad \text{(I)}$$

$$\text{The cumulative drug release} = \frac{Q_n}{Q_0} \times 100\ \% \quad \text{(II)}$$

At time n, $Q_n$ signifies the aggregate discharge of the test material. Concurrently, $C_n$ denotes the quantitatively measured concentration of the sample solution at iteration n, whereas $V_n$ represents the total volume of the recipient pooll; $C_i$ is the measured concentration of the i-th test solution; $Q_o$ is the gallic acid content in QIG-pH-TSG.

#### 2.5.2. Gel morphology property

A scanning electron microscope (SEM), specifically the Zeiss SIGMA model from the United Kingdom, was utilized to conduct an analysis of the structural composition of the QIG-pH-TSG gels. Prior to the SEM analysis, the gels underwent a rigorous preparatory procedure which involved snap-freezing, pulverization, lyophilization, and finally, the application of a gold coating.

#### 2.5.3. Rheological property

The rheological examination of the hydrogels was conducted using a Malvern Kinexus rheometer (England), equipped with a parallel plate geometry of 40 mm diameter. The solutions of the gel precursors were carefully dispensed onto the parallel plates, which were spaced 0.5 mm apart. Subsequently, to determine the storage modulus ($G'$) and loss modulus ($G''$), oscillatory rheological measurements were performed as the temperature of the plates was gradually increased from 4 to 37 °C at a rate of 1 °C·min$^{-1}$. This was followed by a stabilization phase of 600 s at 37 °C.

#### 2.5.4. DSC property

DSC analysis was conducted on P407, P188, HPMC, ethanol extracts of QIG, blank gels, and QIG-pH-TSG. Each sample (5 mg) was carefully placed in a standard aluminum crucible and hermetically sealed. Upon conducting a scan of the crucibles, Differential Scanning Calorimetry (DSC) curves were obtained within a temperature range of 15–440 °C, with a heating rate of 10 °C/min.

#### 2.5.5. Studies of sol dynamics

A slide was inclined at a 45-degree angle at room temperature for 5 min. Subsequently, 40 μL of sample was dispensed onto two glass plates. The time taken for each droplet of sol to slide off a specific distance was measured to plot the time-slip displacement curve, known as the sol kinetic curve.

### 2.6. The in vitro anti-inflammatory of QIG-pH-TSG

RAW264.7 (Xiangya Central Laboratory Cell Bank, Central South University, Changsha, China), was cultured using high-glucose DMEM medium supplemented with 10 % fetal bovine serum (FBS) (10099141C, Gibco, USA), 100 U/mL penicillin, and 100 μg/mL streptomycin (SV30010, HyClone, USA). This cell line is maintained in a 37 °C, 5 % $CO_2$ humidified incubator.

After an overnight culture in a 96-well plate with $2 \times 10^5$ cells per well and 100 μL medium per well, the cells were subjected to treatment with varying concentrations of blank gel (0.05, 0.2, 0.4, 1 mg/mL), QIG-pH-TSG (0.05, 0.2, 0.4, 1 mg/mL), and LPS (1 μg/mL) for a duration of 24 h. Following this treatment period, 10 μL of CCK-8 solution (Titan, Shanghai, China) was added to each well, and the plates were maintained at 37 °C for 4 h. The absorbance of each well was then recorded at 450 nm using a microplate reader (BioTek XS2, USA).

After an overnight incubation period in a 96-well plate, with a cell density of $2 \times 10^5$ cells per well and 100 μL of medium per well, the cells were subjected to a 1-h treatment with a blank gel and various concentrations of QIG-pH-TSG (0.05, 0.2, 0.4, 1 mg/mL). Following this, the cells were treated with LPS for an additional 24 h. After the completion of the experiment, the supernatant from

each well was collected for the purpose of evaluating the concentrations of TNF-α, IL-6, and IL-10 using ELISA kits sourced from Boatman, Shanghai, China. This evaluation was carried out in accordance with the manufacturer's instructions.

### 2.7. In vivo evaluation of DSS induced UC in mice

#### 2.7.1. Animals

64 male Kunming mice aged 6 ~ 8 weeks (20 ± 2 g), was procured and housed within the SPF-classified facility of the Animal Centre at Xinjiang Medical University, which holds a valid license under the number SCXK (Xin) 2023–0001. The experimental procedures and protocols were formally endorsed by the Animal Ethics Review Board of Xinjiang Medical University, with an approval number of LACUC-20210424-29.

#### 2.7.2. Establishment of UC model and grouping

After a period of one week for acclimatization, the mice underwent a process of random allocation into distinct groups: normal control (NC, n = 8), ulcerative colitis model (UC, n = 8), 5-aminosalicylic acid treatment (PC, n = 8), blank gel control (BG, n = 8), and low, medium, and high-dose QIG-pH-TSG treatment groups (QIG-L, QIG-M, QIG-H, n = 8). To induce the UC model, the drinking water of the mice was supplemented with DSS (3 % w/v) for a duration of 14 days. The treatment regimens were as follows: NC and UC groups received distilled water; PC group received 0.3 mg/g of 5-aminosalicylic acid (5-ASA); BG group received 40 mg/mL blank gel; QIG-L, QIG-M, and QIG-H groups received 0.15, 0.3, and 0.6 mg/g of QIG-pH-TSG gel, respectively. All treatments were administered via daily oral gavage for a period of seven consecutive days. Daily evaluations of the mice were systematically conducted, utilizing the disease activity index (DAI) as detailed in Table S1. As previously stated in Ref. [23], the DAI score was determined on a scale spanning from 0 to 4.

#### 2.7.3. Colon length, colon index and CMDI score

The entire colon was excised and placed on a panel for measurement of its length. It was then rinsed with a 0.9 % sodium chloride solution and dried using filter paper. Subsequently, the wet mass of the colon was recorded, and the colon index was calculated as follows: colon index = (weight of colon/body weight) × 100 %. The degree of colonic mucosal damage was assessed according to the colonic mucosal injury index (CMDI) grade and the scoring criteria [24] detailed in Table S2. The remaining colon tissue was preserved at −80 °C for further experiments.

#### 2.7.4. Histopathological observation and scoring

After euthanasia, colon tissues underwent extraction and were then cleansed with chilled PBS. Following this, they were preserved in 10 % neutral buffered formalin. Subsequently, the tissue samples were embedded in paraffin, sliced into 5 μm sections, stained with hematoxylin and eosin (HE), and meticulously examined under an Olympus BX53 light microscope located in Japan. The histological assessment was carried out in accordance with the scoring standards outlined in Table S3 [25], taking into consideration the severity of inflammation, the extent of crypt damage, and the erosion of mucosal layers.

#### 2.7.5. Detection of inflammatory biomarkers

Using the appropriate ELISA kit, measurements were conducted to determine the concentrations of inflammatory agents (IL-6, IL-10, TNF-α) and the inflammatory reactive protein (CRP) present within bodily tissues.

### 2.8. Statistical analysis

Data were expressed as Mean ± SD and analyzed by SPSS 27.0 software, one-way ANOVA was used for comparison between multiple groups, with $P < 0.05$ as the difference being statistically significant.

## 3. Results and discussion

### 3.1. Preparation, and physicochemical characterization of the composite gels

#### 3.1.1. Preparation of the composite gels

In the study, a pH/thermosensitive gel containing QIG (QIG-pH-TSG) was successfully prepared to treat UC. Before the phase transition temperature (34 °C), QIG-pH-TSG appeared as a clear, yellow-brown and homogeneous solution with good fluidity.

**Table 1**
Quality evaluation of thermosensitive gel samples.

| Batch no. | pH | Gelation temperature (°C) | Viscosity (mPa.s) | |
|---|---|---|---|---|
| | | | 4 °C | 25 °C |
| 1 | 4.94 ± 0.03 | 33.40 ± 0.21 | 0.81 ± 0.07 | 1044.3 ± 0.7 |
| 2 | 4.99 ± 0.04 | 34.04 ± 0.33 | 0.89 ± 0.05 | 1075.1 ± 0.9 |
| 3 | 4.90 ± 0.06 | 33.04 ± 0.57 | 0.82 ± 0.08 | 1086.5 ± 0.8 |

However, when the phase transition temperature is reached, it turns into a transparent, uniform, and elastic yellow-brown semisolid.

The evaluation of an intestinal formulation is heavily reliant on the quality of the preparation. The pH of the QIG-pH-TSG, in conjunction with its gelation temperature and viscosity (as detailed in Table 1), falls within the acceptable range for administration (5.0–9.0). At a colon temperature of 34 °C, the gel underwent a transition from a liquid to a semi-solid state. Furthermore, following a 14-day storage period at both ambient temperature (25 °C) and physiological temperature (37 °C), the results of centrifugation indicated an absence of stratification, thereby confirming the consistent characteristics of the samples.

### 3.1.2. Release behaviors of QIG-pH-TSG

The *in vitro* release profile of active ingredients serves as a valuable predictor of the pharmaceutical and therapeutic potential of formulations [26]. The present study conducted an assessment of the *in vitro* emission of the formulated gel, designated as QIG-pH-TSG, utilizing artificial gastric, intestinal, and colon fluids, as depicted in Fig. 1. The cumulative release rate of QIG-pH-TSG showed sustained release kinetics, reaching a maximum of 102.16 ± 2.92 % over 24 h. Notably, the release of the gel in artificial colon fluid differed significantly from that in artificial gastric and intestinal fluids at the 24-h mark ($P < 0.01$). A variety of mathematical models, encompassing Zero-order, First-order, Higuchi, and Ritger-Peppas models, were employed to correlate with the release data obtained from the QIG-pH-TSG system, with results summarized in Table S4. The cumulative release rate ($Y = 118.82889\ (1\text{-}e^{-0.07287t})$, $R^2 = 0.99195$) displayed a strong linear relationship with time, indicating zero-order kinetic processes. Thus, complete release of QIG-pH-TSG was achieved within 24 h, while maintaining gel temperature and viscosity within specified parameters, prompting further investigation into other physicochemical properties.

### 3.1.3. Microstructure of QIG-pH-TSG

The gel surface's microstructure and pore dimensions were examined using scanning electron microscopy (SEM), with various levels of magnification being applied to obtain detailed insights. The blank gel (Fig. 2 A1- A3) exhibited numerous circular holes with a loose lamellar structure and a large number of through-holes, showing a uniform, grid-like porous network. In the drug-loaded gel (Fig. 2 B1-B3), the aqueous extract of QIG was uniformly dispersed within the gel matrix, filling its pores. The microscopic images clearly demonstrate the successful incorporation of QIG into the gel matrix, resulting in the efficient filling of its pores. Furthermore, this integration is suggested to potentially enhance the efficacy of the QIG-pH-TSG system, as evidenced by the microstructural imagery.

### 3.1.4. Rheological of QIG-pH-TSG

At 4 and 25 °C, the shear stress (σ) of QIG-pH-TSG increased linearly with the shear rate (γ), while the viscosity (η) remained constant, indicating Newtonian fluid behavior. However, at 37 °C, although σ tends to stabilize, η decreased with increasing γ, indicating pseudoplastic fluid behavior (Fig. 3A and B). At 4 and 25 °C, the QIG-pH-TSG curves showed no peak, suggesting the samples did not exhibit yield stress (Fig. 3C and D). This indicated Newtonian fluid behavior, flowing freely without requiring external force. At 37 °C, the curve showed an initial rise followed by a decline with a distinct peak, suggesting gel formation and a requirement for a certain stress level to induce flow. This implies the sample might exhibit some degree of retention at the drug administration site.

Viscosity depends not only on shear rate but also on time. Materials with thixotropic properties typically exhibit shear thinning, though shear-thinning materials may not always possess thixotropic properties. Thixotropy is crucial for understanding test results repeatability. At 4 °C, η remained constant with increasing γ, indicating Newtonian fluid without shear thinning. At 25 and 37 °C, the QIG-pH-TSG exhibited clear shear thinning behavior and quickly returned to its original state after high-intensity shear. Thus, QIG-pH-TSG does not exhibit thixotropy, and viscosity-time relationships could be quantified through thixotropy testing. Results showed that viscosity in QIG-pH-TSG remained unaffected by time (Fig. 3 D).

G′ assesses the stability of the material's structure, while G″ indicates viscous or flow characteristics. Unchanged G′ suggests material integrity. Subsequent tests must be conducted within the linear viscoelastic region. At 4 and 25 °C, G″ > G′ and δ > 45° of QIG-pH-TSG suggested fluidic characteristics (Fig. 3E and F). At 37 °C, the γ* <1 %, G′ > G″ and δ < 45° indicated a gel structure. As γ* >1 %, both G′ and G″ declined, while δ increased, signifying complete disruption of the gel structure. Thus, γ* should be maintained below 1

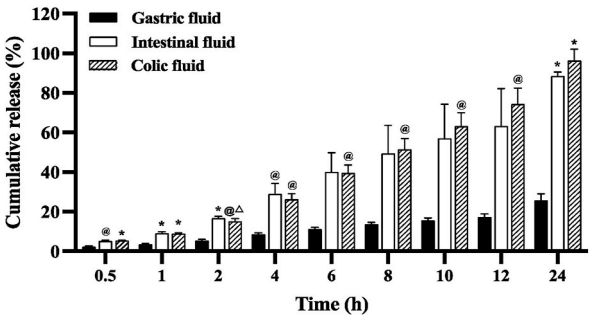


**Fig. 1.** Cumulative release of QIG-pH-TSG prescription in different release media. Compared with the cumulative release in gastric fluid, $^{*}P < 0.01$, $^{@}P < 0.05$. Compared with the cumulative release in intestinal fluid, $^{\#}P < 0.01$, $^{\triangle}P < 0.05$.

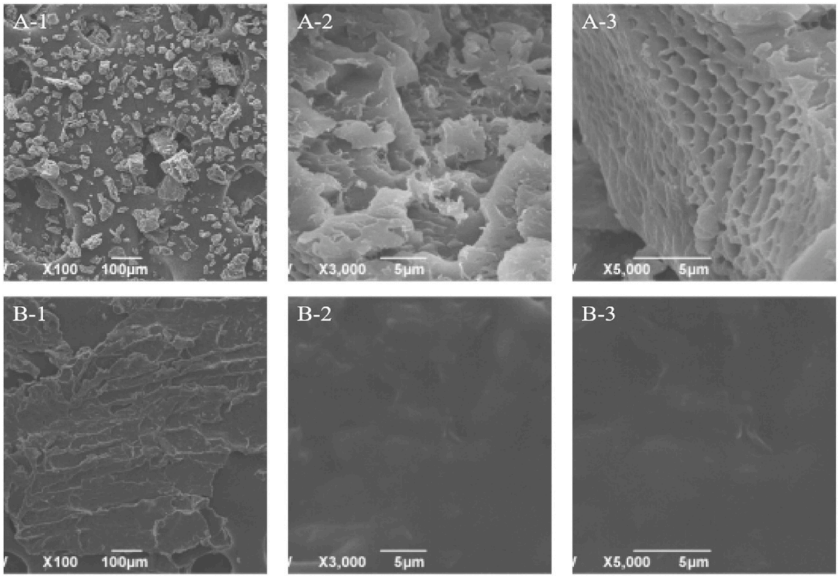


**Fig. 2.** SEM plots of blank gel (A-1, A-2 and A-3) and QIG-loaded gel (B-1, B-2 and B-3).

% in dynamic oscillation experiments.

At temperatures ranging from 4 to 25 °C, the value of G″ consistently surpasses that of G′, with δ notably exceeding 45°, a clear indication of substantial viscous reactions occurring. When the temperature is set to 37 °C, both G′ and G″ exhibit an approximately fourfold increase in their respective values. Notably, under these conditions, G′ surpasses G″, while δ decreases to a level below 45°, revealing distinct elastic characteristics with minimal frequency dependence, signifying a stable cross-linked structure (Fig. 3G and H).

As the temperature escalated, there was a notable augmentation in G′, G″, and η* values, while δ decreased. Around 32 °C, G′ intersected with G″, marking the phase transition temperature. Prior to this transition, G″ exceeded G′, with lower η* and δ > 45°, indicating evident fluid properties. After the transition, G′ surpassed G″, η* sharply increased, and δ dropped below 45°, indicating gel formation (Fig. 3I–K). G′, G″, η*, and δ then stabilized, suggesting that while QIG-pH-TSG underwent a phase transition, it did not fully solidify with high hardness, thus not impeding drug release.

### *3.1.5. DSC of QIG-pH-TSG*

For the purpose of thoroughly examining the thermal properties of the drug and gels, DSC graphs were generated (as depicted in Fig. 4). The DSC curve of QIG ethanol extract exhibited peaks between 150 and 350 °C (Fig. 4 E), with complex peaks in the 200–350 °C range due to the complexity of the QIG crude extract, manifesting various thermal behaviors such as crystallization, melting, glass transition, curing, and degradation. In the DSC curve of the blank gel (Fig. 4 F) showed two distinct endothermic peaks (61.8 °C) similar to the excipients P407 (Fig. 4 A) and P188 (Fig. 4 B), likely due to matrix melting, whereas SA and HPMC showed broad endothermic peaks at 40–120 °C (Figs. 4C) and 40–100 °C (Fig. 4 D), respectively. A separate peak at higher temperatures (278.6 °C) possibly indicated matrix degradation. The DSC curve of QIG-pH-TSG (Fig. 4 G) showed two sharp endothermic peaks around 60.7 and 338.9 °C. Compared to the blank gel's peaks (61.8 and 278.6 °C), the latter peak shifted to 338.9 °C within the range of QIG's endothermic peak (150–350 °C), suggesting enhanced thermal stability of the gel with QIG addition.

### *3.1.6. Studies of QIG-pH-TSG in sol dynamics*

The non-ionic triblock copolymers, namely P407 and P188, consist of polyoxyethylene (PEO) segments that exhibit hydrophilic properties, as well as polyoxyethylene (PPO) segments that demonstrate hydrophobic characteristics, with these components present in varying mass ratios [27]. Based on the theory of inter-micelle entanglement and stacking, QIG-pH-TSG exhibited a longer duration to traverse the same sliding distance compared to the blank gel (Fig. 5A and B). This suggested that the inclusion of QIG ethanol extract resulted in tighter wrapping of water molecules around the PEO block, rendering them more resistant to detachment, and enhancing adhesion. Therefore, P407 and P188 were effectively used to formulate QIG-pH-TSG, aiming to prolong its effects in the colon.

## *3.2. The in vitro anti-inflammatory effect of QIG-pH-TSG in RAW264.7*

The *in vitro* observation of RAW264.7 cells has revealed the anti-inflammatory properties of QIG-pH-TSG. In comparison to the normal control group, the proliferation of RAW264.7 cells remained unaffected by both the blank gel and QIG-pH-TSG at concentrations ranging from 0.05 to 1 mg/mL. Thus, subsequent experiments were conducted using the concentration range of 0.05, 0.2, 0.4, and 1 mg/mL (Fig. 6 A). Compared to the normal control group, the LPS group showed a significant increase ($P < 0.001$) in the secretion of TNF-α and IL-6 (Fig. 6B–D). In contrast to the LPS model group, all four concentrations of QIG-pH-TSG (0.05, 0.2, 0.4, 1

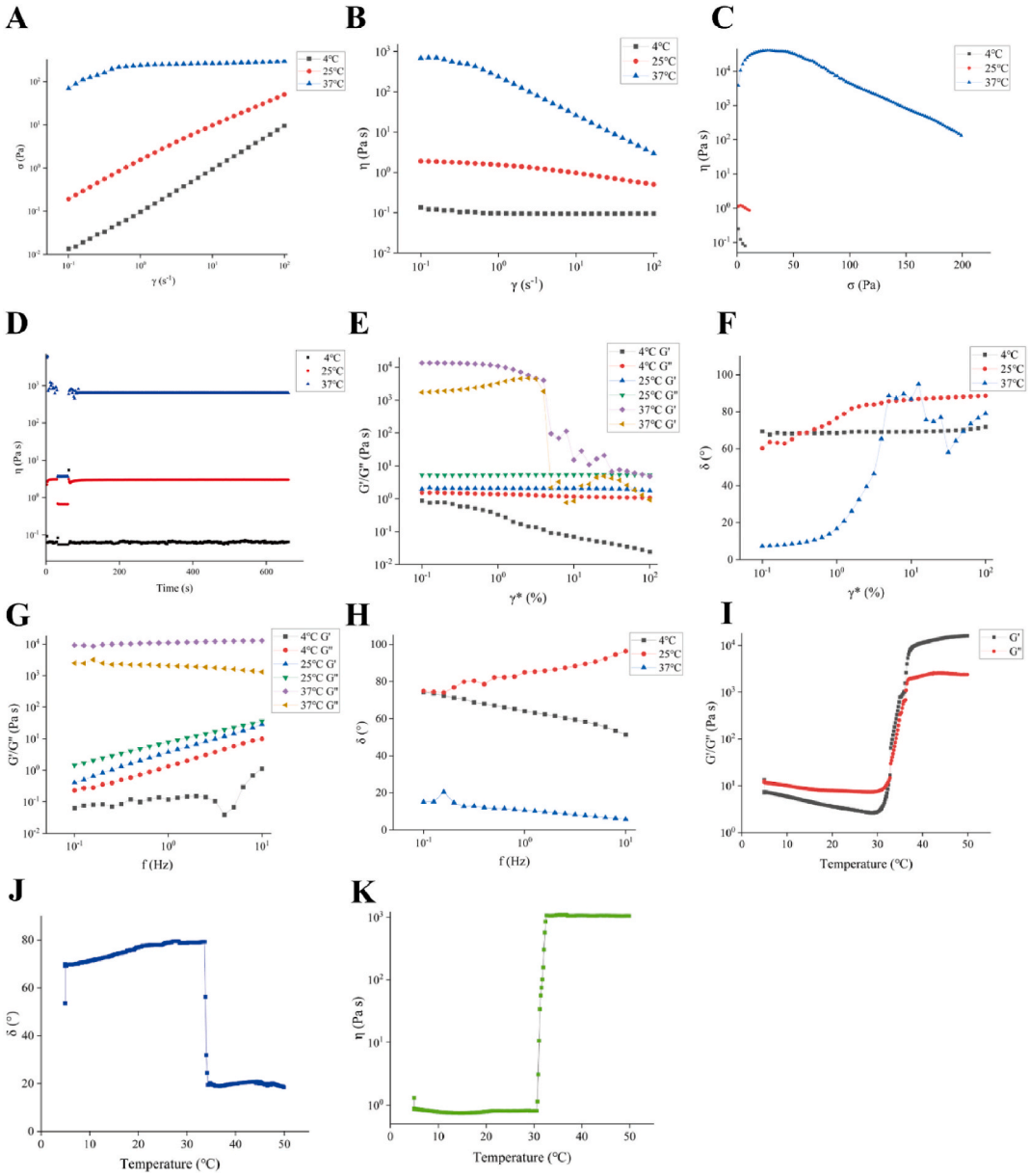


**Fig. 3.** Rheological properties of QIG-pH-TSG. Variation curves of γ versus η and σ at different temperatures (**A** and **B**); Variation curves of σ vs η at different temperatures (**C**); Variation curves of step shear rate γ and η with time for different temperatures (**D**); Variation curves of γ* versus G′, G″, and δ at different temperatures (**E** and **F**); Variation curves of G′, G″ and δ with different f (**G** and H); Variation curves of G′, G″, η* and δ in the programmed temperature increase (**I–K**).

mg/mL) resulted in a notable decrease in TNF-α and IL-6 production, accompanied by a marked elevation in IL-10 levels ($P < 0.001$). Notably, the absence of QIG in the empty gel did not lead to a reduction in TNF-α and IL-6 production or an increase in IL-10 levels, indicating that the anti-inflammatory effects of QIG-pH-TSG are attributed to the presence of QIG. This suggests that QIG-pH-TSG possesses potential anti-inflammatory properties *in vivo* by modulating the relevant inflammatory mediators.

### *3.3. Therapeutic effects of QIG-pH-TSG in UC mice induce by DSS*

#### *3.3.1. Effects on DAI, the length, weight and index of colon and CMDI*

Mice subjected to DSS-induced conditions exhibited weight loss, resulting in an increase in Disease Activity Index (DAI). The DAI scores of QIG-pH-TSG across the three dosage groups displayed dose-dependent changes, as presented in Table 2. DAI scores increased with weight loss during the modeling phase and decreased with symptom relief during interventions with QIG-pH-TSG. In comparison

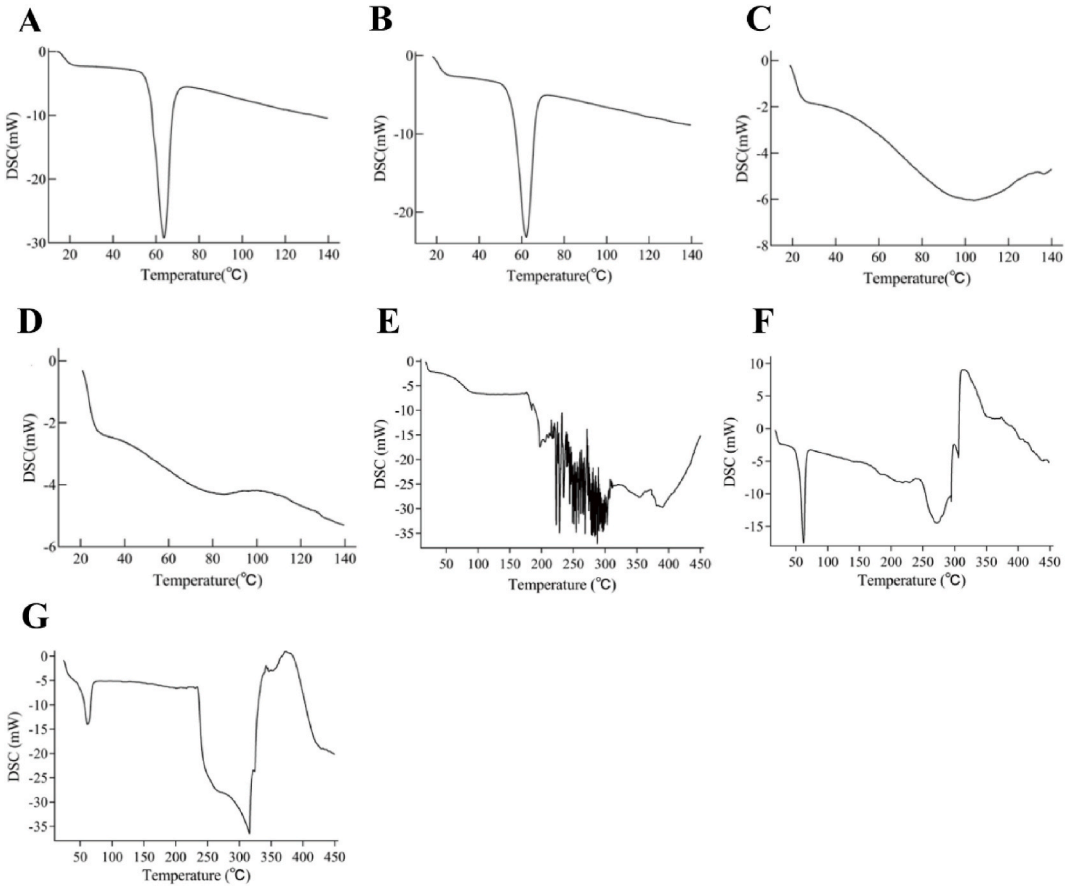


**Fig. 4.** The DSC curves of P4017 (A), P188 (B), SA (C), HPMC (D). DSC curves of QIG ethanolic extracts (E), blank gels (F) and QIG-pH-TSG (G).

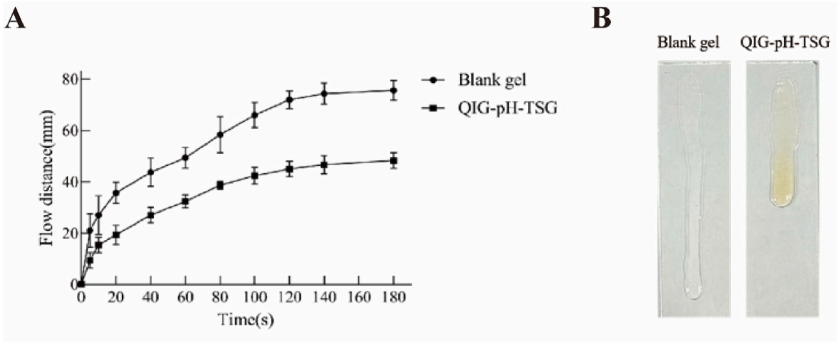


**Fig. 5.** Sliding distances of QIG-pH-TSG (A) and blank gels after 3 min (B).

to the normal group, the DAI score of the model group was 8.500 ± 1.195 by day 14, the results demonstrated a statistically significant increase ($P < 0.01$), confirming the successful induction of UC via DSS. Following a period of two weeks of treatment, the QIG-pH-TSG group exhibited a marked reduction in DAI scores compared to the model group ($P < 0.01$), suggesting an alleviation of symptoms subsequent to the administration of QIG-pH-TSG.

Fig. 7A demonstrated that the colon length of the model group measured approximately 10 cm, which was significantly shorter ($P < 0.01$) in comparison to the 13.6 cm observed in the standard group. Additionally, there was a considerable decrease in colon weight ($P < 0.01$) and colon index ($P < 0.01$) when compared to the control group, indicating potential damage to colon tissue as a result of DSS exposure. Furthermore, the model group displayed a significantly elevated Colon Mucosal Damage Index (CMDI) score ($P < 0.01$) when compared to the normal group, suggesting that DSS modeling caused colon damage. After a period of two weeks of QIG-pH-TSG therapy, a notable increase in colon length was observed, wet mass and index, along with a decrease in CMDI in the QIG-pH-TSG

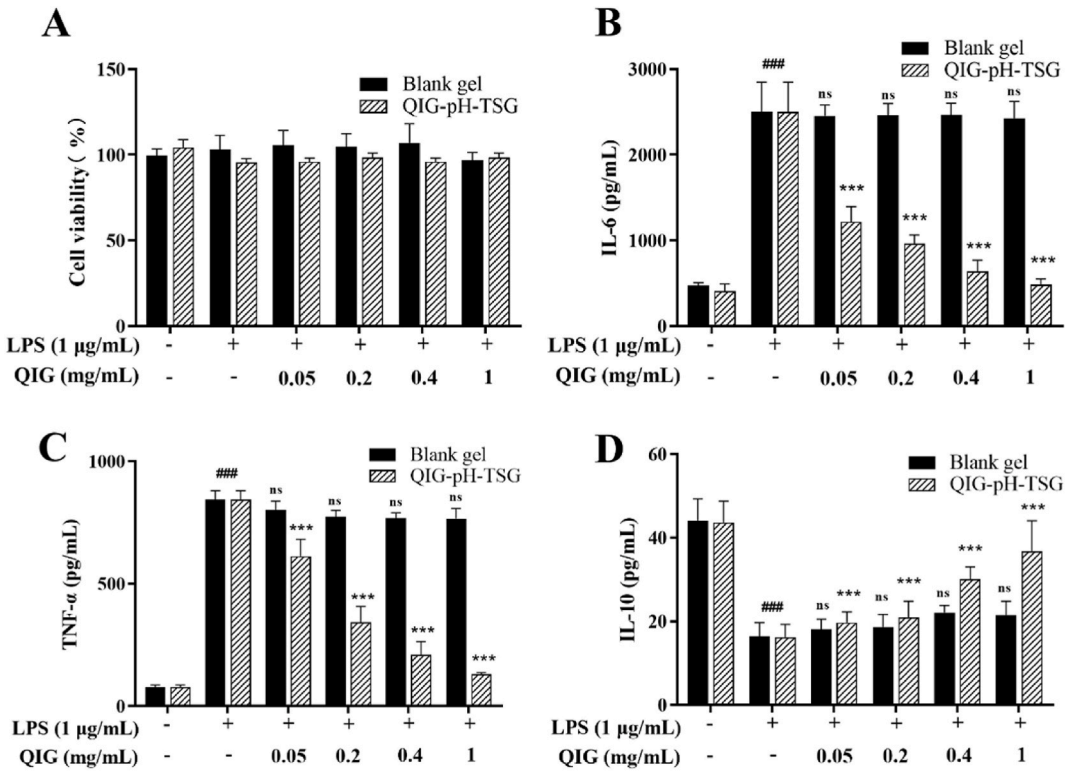


**Fig. 6.** Effect of QIG-pH-TSG on LPS-induced inflammatory factors in the supernatant of RAW264.7 cells. Cell viability (**A**), IL-6 (**B**), TNF-α (**C**) and IL-10 (**D**) were detected by ELISA. Compared with the normal group, $^{\#}P < 0.05$, $^{\#\#}P < 0.01$, $^{\#\#\#}P < 0.001$. Compared with the LPS group, $^{*}P < 0.05$, $^{**}P < 0.01$, $^{***}P < 0.001$.

**Table 2**
The results of disease activity index (DAI) of mice on day 1, 7 and 14.

| Groups | Day 1 | Day 7 | Day 14 |
|---|---|---|---|
| Normal | 0.000 ± 0.000 | 0.000 ± 0.000 | 0.000 ± 0.000 |
| Model | 9.625 ± 0.916$^{\triangle}$ | 9.125 ± 0.835$^{\triangle}$ | 8.500 ± 1.195$^{\triangle}$ |
| Bank gel | 9.625 ± 0.744$^{\triangle}$ | 9.000 ± 1.512$^{\triangle}$ | 8.000 ± 1.309$^{\triangle}$ |
| QIG suspension | 9.500 ± 0.926$^{\triangle}$ | 6.250 ± 0.707$^{\triangle\#}$ | 5.375 ± 0.744$^{\triangle\#}$ |
| QIG-pH-TSG-L | 9.500 ± 0.535$^{\triangle}$ | 5.875 ± 0.991$^{\triangle\#}$ | 4.625 ± 0.518$^{\triangle\#}$ |
| QIG-pH-TSG-M | 9.625 ± 1.061$^{\triangle}$ | 5.125 ± 1.458$^{\triangle\#}$ | 4.000 ± 1.069$^{\triangle\#\&\&}$ |
| QIG-pH-TSG-H | 9.500 ± 1.773$^{\triangle}$ | 4.500 ± 1.309$^{\triangle\#\&*}$ | 3.625 ± 1.061$^{\triangle\#\&*}$ |
| Positive | 9.625 ± 1.061$^{\triangle}$ | 4.250 ± 1.282$^{\triangle\#\&*}$ | 3.875 ± 1.458$^{\triangle\#\&\&}$ |

Compared with the normal group, $^{\triangle}P < 0.01$. Compared with the model group, $^{\#}P < 0.01$. Compared with the QIG suspension group, $^{\&}P < 0.01$, $^{\&\&}P < 0.05$. Compared with the QIG-pH-TSG-L group, $^{*}P < 0.05$.

medium- and high-dose groups (Fig. 7A–E). These findings demonstrated that the model group mice displayed physical symptoms and colonic pathological characteristics resembling those of human UC, the reported symptoms include significant weight loss, diarrhea, bloody stools, and an elevated level of colonic damage index, colon shortening, and colonic damage. QIG-pH-TSG effectively alleviated these symptoms with sustained efficacy, highlighting the therapeutic superiority of the formulated gel in managing UC.

### *3.3.2. QIG-pH-TSG alleviated the colon injury in UC mice*

This study entailed the induction of Ulcerative Colitis (UC) in mice through a prescribed two-week administration of a 3.5 % DSS solution in water. To investigate the effects of QIG-pH-TSG on colonic mucosa epithelial injury, histopathological scoring was performed across different experimental groups. As illustrated in Fig. 8 A, within the standard group, a systematic arrangement of intestinal mucosal cells and crypts is observed, notable for the prominent presence of cup cells. In contrast, model mice showed severe damage to intestinal mucosal epithelial cells, disorganized glandular structures, reduced cup cells, and extensive crypt damage. In the process of evaluating the inflammatory cell infiltration within the mucosal and muscular layers, it was observed that the scores were significantly higher compared to those in the normal group ($P < 0.01$), thereby confirming the successful establishment of the UC model. Conversely, when examining the crypts in the QIG-pH-TSG group, a heightened degree of organizational structure was evident,

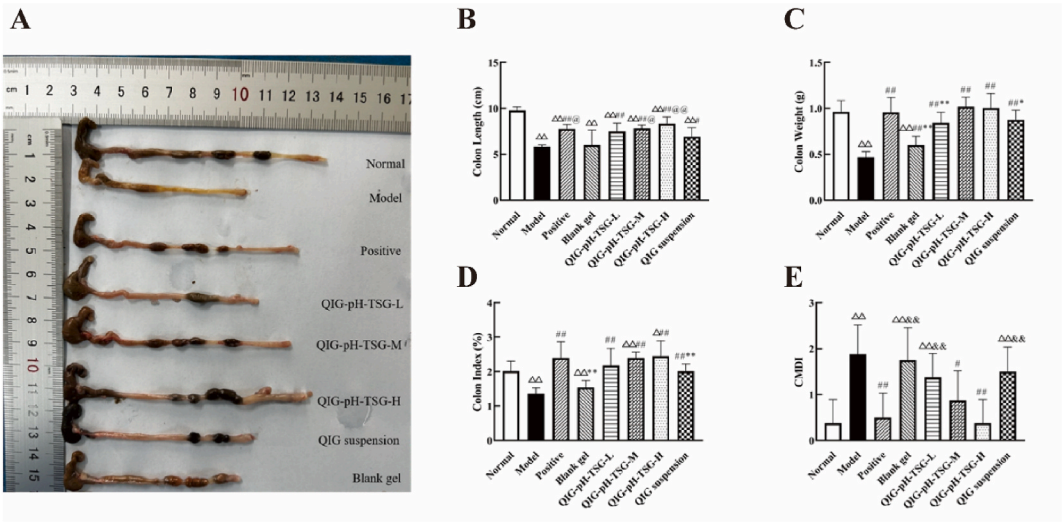


**Fig. 7.** Effect of QIG-pH-TSG on colon length, weight, index and CMDI score. Compared with the normal group, $^{\triangle}P < 0.05$, $^{\triangle\triangle}P < 0.01$. Compared with the model group, $^{\#}P < 0.05$, $^{\#\#}P < 0.01$. Compared with the QIG-pH-TSG-M group, $^{*}P < 0.05$, $^{**}P < 0.01$. Compared with the QIG suspension group, $^{@}P < 0.05$, $^{@@}P < 0.01$. Compared with QIG-pH-TSG-H group, $^{\&}P < 0.05$, $^{\&\&}P < 0.01$.

characterized by a diminished space between the crypt's foundation and the mucosal muscular layer. Furthermore, the colonic tissue damage scores were notably lower than those recorded in the model group ($P < 0.01$), indicating that the administration of the drug effectively mitigated colonic tissue damage, particularly in the low-dose QIG-pH-TSG group (Fig. 8 B).

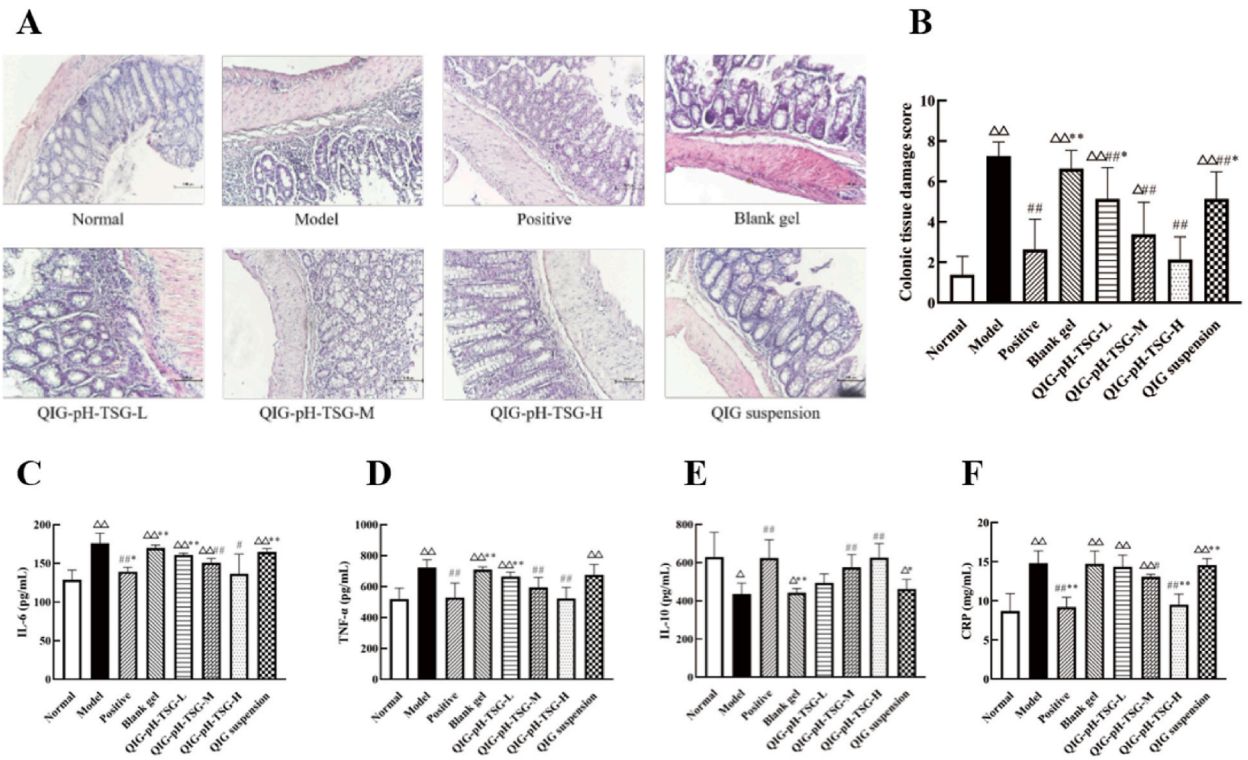


**Fig. 8.** Effect of QIG-pH-TSG in colonic tissue damage and inflammation of UC mice induced by DSS. (A–B) Colonic tissue damage; (C–F) levels of IL-6, TNF-α, IL-10 and CRP in the colonic tissues of mice. Compared with the normal group, $^{\triangle}P < 0.05$, $^{\triangle\triangle}P < 0.01$. Compared with the model group, $^{\#}P < 0.05$, $^{\#\#}P < 0.01$. Compared with the QIG-pH-TSG medium-dose group, $^{*}P < 0.05$, $^{**}P < 0.01$.

### 3.3.3. Effects of QIG-pH-TSG on inflammatory biomarkers and mediators in UC mice

UC is characterized by an inflammatory response influenced by various etiological factors. IL-6, TNF-α, and IL-10 are pivotal cytokines involved in the inflammatory process. The concentrations of IL-6 and TNF-α positively correlate with the severity of inflammation in the body, whereas IL-10 exhibits an inverse correlation [28]. As illustrated in Fig. 8C–E, a notable elevation in the levels of IL-6 and TNF-α was observed in the colon tissues of the model group compared to the normal group ($P < 0.01$), accompanied by a significant decrease in IL-10 levels ($P < 0.05$), confirming the effective induction of the model and evident inflammatory damage in the mouse colon. Following a two weeks administration, a notable reduction in colon IL-6 levels was recorded in both the positive control ($P < 0.01$) and high-dose (QIG-pH-TSG-H) groups ($P < 0.05$), in contrast to the control group. Furthermore, there was a significant decrease in TNF-α levels in the colon of both the high-dose ($P < 0.01$) and positive control groups ($P < 0.01$). Additionally, a notable increase in IL-10 levels was observed in the colon of QIG-pH-TSG-H ($P < 0.01$), indicating that the administration of QIG-pH-TSG mitigated systemic inflammation in the colons of UC mice.

C-reactive protein (CRP) is the most widely recognized protein in the acute phase [24], with clinical assessments demonstrating a robust correlation between CRP concentrations and UC [29]. As depicted in Fig. 8 F, the CRP levels in the colon tissue of the model group were significantly elevated compared to those in the normal group ($P < 0.01$), confirming the effective induction of the UC model using DSS. Conversely, a notable reduction in colon CRP levels was observed in both the QIG-pH-TSG-H group ($P < 0.01$) and the positive drug control group ($P < 0.01$), relative to the control group. These findings indicate that QIG-pH-TSG possesses the ability to decrease C-reactive protein levels, thereby alleviating colonic inflammation.

### 3.3.4. Antioxidant effects of QIG-pH-TSG in UC mice

Reactive oxygen species (ROS) have been shown to damage the mucosal layer of the gastrointestinal tract, triggering immune responses and leading to inflammatory bowel disease, including UC [30]. As shown in Fig. 9, there was a marked decrease in SOD levels observed in the tissues of the model group, accompanied by a significant increase in MPO levels when compared to the normal group ($P < 0.01$). Across all dosage groups of QIG-pH-TSG, there was an elevation in SOD levels (Fig. 9 A) and a corresponding decrease in MPO expression (Fig. 9 B) when compared to the model group ($P < 0.05$, $P < 0.01$). Following QIG-pH-TSG administration, SOD levels improved, and MPO levels decreased, indicating that QIG-pH-TSG could regulate oxidative stress and reduce oxidative damage in UC mice.

## 4. Discussion

Recently, there has been a consistent increase in the incidence of UC, which has paralleled improvements in living standards. The pathogenesis of UC is multifaceted, involving persistent inflammatory responses due to mucosal barrier alterations, dysregulation of intestinal flora, and immune system deficiencies. The severity and persistence of these factors correlate with the morbidity and mortality rates associated with UC. DSS, a water-soluble polysaccharide, it exerts a direct detrimental effect on the epithelial cells of the intestinal mucosa, thereby compromising the integrity of the intestinal barrier. DSS-induced colitis in animal models closely resembles human UC in terms of histological features and inflammation distribution, making it a popular choice for creating UC models in research. In this study, the induction of UC in mice was accomplished through the administration of a 3.5 % DSS, which the mice were allowed to consume freely for a period of two weeks. The results indicated that the model group mice exhibited physical signs and colonic pathological manifestations similar to human UC symptoms, examples encompass notable weight loss, the manifestation of diarrheal symptoms or the presence of fecal blood, as well as an increase in the colonic damage index, splenic weight coefficient, colon shortening, and colonic damage. Amino salicylic acid drugs, including 5-ASA, are non-specific anti-inflammatory agents that temporarily control and alleviate UC symptoms. Due to their precise efficacy and cost-effectiveness, they remain the first-line

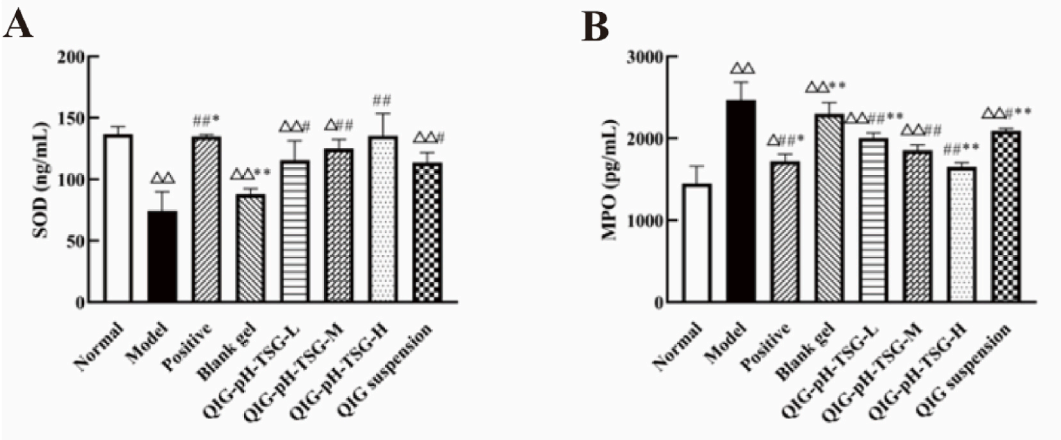


**Fig. 9.** Levels of SOD and MPO in colonic tissues of UC mice induced by DSS. Compared with the normal group, $^{\triangle}P < 0.05$, $^{\triangle\triangle}P < 0.01$. Compared with the model group, $^{\#}P < 0.05$, $^{\#\#}P < 0.01$. Compared with the QIG-pH-TSG medium dose group, $^{*}P < 0.05$, $^{**}P < 0.01$.

treatment for UC. As a result, 5-ASA was chosen as the positive control medication for this study, ensuring a rigorous and scientific approach to the experimental design.

In traditional Chinese medicine (TCM), QIG is characterized as bitter in taste, warm in nature, with effects believed to influence the lungs, spleen, and kidneys. It is recognized for its ability to regulate "Qi", "Essence", "Lungs", and "Bleeding", making it a commonly used remedy for inflammatory disease. The primary constituent of QIG is gallic acid, which has been discussed in numerous studies [31]. Gallic acid (GA) possesses a broad spectrum of biological activities, including antioxidant, anti-inflammatory and anti-mutagenic. It also demonstrates anti-tumorigenic effects by inhibiting metastasis and prolonging the survival of mast cell tumors. Despite the existence of laboratory research that has verified the anti-inflammatory properties and mechanisms of QIG *in vitro* [32], there is a paucity of documentation on its anti-inflammatory and antioxidant effects *in vivo*, particularly concerning UC. Therefore, after successful preparation of QIG-PH-TSG, we first examined its therapeutic effect by establishing a UC model and evaluating relevant indicators such as colon function, inflammatory response, and antioxidation properties.

UC is characterized by an inflammatory response mainly influenced by such cytokines IL-6, TNF-α, and IL-10. Levels of IL-6 and TNF-α positively correlate with the extent of inflammation in the body, while IL-10 exhibits the opposite trend [33]. Elevated concentrations of pro-inflammatory cytokines, including IL-6 and TNF-α, contribute to significantly to the pathogenesis of UC, whereas IL-10 exerts an anti-inflammatory effect. C-reactive protein (CRP), a crucial component of the innate immune system, is predominantly synthesized by the liver and functions to regulate inflammatory responses [25]. Elevated CRP levels serve as valuable biomarkers for the diagnosis and prognosis of UC treatment outcomes [34]. Studies have demonstrated that heightened CRP levels serve as a robust indirect marker of severe ulceration in UC, thereby influencing the choice of therapeutic interventions [35]. Furthermore, modulating the Treg/Th17 balance in a gut microbiota-dependent manner can effectively mitigate colonic inflammation [36].

An imbalance in the body's oxidative and antioxidant systems gives rise to oxidative stress (OS) [37]. In situations of OS, the accumulation of reactive oxygen species (ROS) can potentially trigger protein dysfunction, lipid peroxidation, and DNA damage, ultimately leading to increased apoptosis [38]. Studies have demonstrated that the colon cells in patients with UC exhibit elevated levels of ROS, including SOD, $H_2O_2$, and HOCl [39]. Additionally, histopathological assessment of neutrophils and macrophages within the intestinal mucosa of UC patients indicates a substantial production of superoxide [40]. Among these, SOD decomposes ROS and scavenges harmful superoxide anion free radicals, thereby measuring the organism's antioxidant capacity [41]. MPO, a hemoprotein, it serves as an operational marker for assessing tissue neutrophils and is correlated with the severity of inflammation observed in UC [42]. It is often upregulated in the inflamed mucous membranes of UC patients, potentially contributing to cancerous transformations.

Our meticulous research has observed a significant elevation in MPO, IL-6, TNF-α, and CRP levels subsequent to the induction of the UC model, coupled with a substantial decrease in SOD and IL-10 levels. This phenomenon implies a sudden and pronounced inflammatory response within the colon following the administration of DSS. Administration of QIG-PH-TSG resulted in a notable reduction in MPO, IL-6, TNF-α, and CRP levels, as well as an augmentation in SOD and IL-10 expression. This indicated that QIG-PH-TSG effectively mitigated inflammation and oxidative damage in UC mice. A comprehensive analysis of the DAI, colon length, spleen coefficient, pathological evaluations, and the expression of pertinent inflammatory factors had revealed that the group receiving a high dose of QIG-pH-TSG exhibited the most potent therapeutic effect on DSS-induced UC in mice. Furthermore, comparable pharmacodynamic outcomes were observed in both the high-dose QIG-pH-TSG group and the group administered with positive control drugs. The gel formulation released QIG locally at the colonic lesion site, increasing drug concentration in the area and providing anti-inflammatory efficacy, thereby enhancing the therapeutic outcome through gel preparation. Our results demonstrated that a PH/sensitive gel formulation was suitable for delivering QIG effectively at the colon site via enema.

Despite the incomplete understanding of the exact mechanism underlying UC, the well-established association between UC and inflammation is widely recognized. QIG-pH-TSG offers significant therapeutic benefits for UC by effectively regulating various indices in UC mice. The observations regarding the use of QIG as an active pharmaceutical ingredient through the preparation of pH-sensitive gel provide an experimental foundation for further research on the treatment mechanisms of UC utilizing QIG-PH-TSG.

## 5. Conclusion

In summary, our physicochemical characterization confirms the successful development of a novel gel, QIG-pH-TSG, endowed with heat and pH sensitivity, along with therapeutic efficacy against UC. This gel exhibited porous, evenly dispersed properties indicative of Newtonian fluid behavior at 4 and 25 °C. However, at 37 °C, it displayed pseudoplastic behavior with a measurable yield stress, maintaining a stable cross-linking structure within the physiological temperature range. QIG-pH-TSG not only could decrease the cytokines level of TNF-α and IL-6, and increase IL-10 in RAW 264.7 actived by LPS, but also could alleviate the inflammation in colon of DSS induced mice. Regarding therapeutic efficacy in UC mice, QIG-pH-TSG effectively reduced pro-inflammatory cytokines (TNF-α, IL-6, CRP), enhanced anti-inflammatory cytokine (IL-10) levels, and exhibited antioxidant properties, thereby shielding mice from DSS-induced damage. Considering these comprehensive findings, QIG-pH-TSG shows promise as a novel therapeutic formulation for UC treatment.

## Ethics declaration

The studies involving laboratory animals were reviewed and approved by the Animal Ethics Review Board of Xinjiang Medical University (Approval No.: LACUC-20210424-29).

## Funding

This work was supported by Xinjiang Key Laboratory of Active Components and Drug release Technology of Natural drugs (XJDX1713) and Xinjiang Medical University Doctoral Research Initiation Fund (201915).

## Data availability statement

All relevant data are within the manuscript and its Additional files.

## CRediT authorship contribution statement

**Jiaojiao Bai:** Writing – original draft. **Yan Ding:** Methodology. **Mubarak Iminjan:** Writing – review & editing. **Kudelaidi Kuerban:** Writing – review & editing.

## Declaration of competing interest

The authors declare the following financial interests/personal relationships which may be considered as potential competing interests: Mubarak Iminjan reports financial support was provided by **X**injiang Key Laboratory of Active Components and Drug release Technology of Natural drugs. Mubarak Iminjan reports financial support was provided by Xinjiang Medical University Doctoral Research Initiation Fund. If there are other authors, they declare that they have no known competing financial interests or personal relationships that could have appeared to influence the work reported in this paper.

## Appendix A. Supplementary data

Supplementary data to this article can be found online at https://doi.org/10.1016/j.heliyon.2024.e36225.

## References

[1] J.P. Segal, J.F. LeBlanc, A.L. Hart, Ulcerative colitis: an update, Clin. Med. 21 (2) (2021) 135–139.
[2] L. Du, C. Ha, Epidemiology and pathogenesis of ulcerative colitis, Gastroenterol Clin North Am 49 (4) (2020) 643–654.
[3] L. Ramos, J. Teo-Loy, M. Barreiro-de Acosta, Disease clearance in ulcerative colitis: setting the therapeutic goals for future in the treatment of ulcerative colitis, Front. Med. 9 (2022) 1102420.
[4] C. Le Berre, S. Honap, L. Peyrin-Biroulet, Ulcerative colitis, Lancet 402 (10401) (2023) 571–584.
[5] T. Nakamura, et al., Current pharmacologic therapies and emerging alternatives in the treatment of ulcerative colitis, Digestion 77 (Suppl 1) (2008) 36–41.
[6] S.Y. Cao, et al., Progress in active compounds effective on ulcerative colitis from Chinese medicines, Chin. J. Nat. Med. 17 (2) (2019) 81–102.
[7] M. Wang, et al., Traditional Chinese Medicine: a promising strategy to regulate the imbalance of bacterial flora, impaired intestinal barrier and immune function attributed to ulcerative colitis through intestinal microecology, J. Ethnopharmacol. 318 (Pt A) (2024) 116879.
[8] Y. Liu, et al., Potential activity of traditional Chinese medicine against ulcerative colitis: a review, J. Ethnopharmacol. 289 (2022) 115084.
[9] Z. Yang, et al., A potential therapeutic target in traditional Chinese medicine for ulcerative colitis: macrophage polarization, Front. Pharmacol. 13 (2022) 999179.
[10] H.X. Sun, Y. Zhu, Progress on regulation of NLRP3 inflammasome by Chinese medicine in treatment of ulcerative colitis, Chin. J. Integr. Med. 29 (8) (2023) 750–760.
[11] R. Khan, et al., α-Terpineol mitigates dextran sulfate sodium-induced colitis in rats by attenuating inflammation and apoptosis, ACS Omega 8 (32) (2023) 29794–29802.
[12] Y.X. Hu, et al., [Gallnut and its identification as a herb in traditional Chinese medicine], Zhonghua Yi Shi Za Zhi 53 (1) (2023) 8–14.
[13] M. Iminjan, et al., [Process of gallnut suppository preparation], Zhongguo Zhongyao Zazhi 42 (16) (2017) 3136–3142.
[14] Therapeutic effect of gallnut aqueous extract on ulcerative colitis in rats, Herald Med. 38 (4) (2019) 435–439.
[15] H. Jin, et al., Preparation, characterization, and performance of a modified polyacrylamide-sericite gel, Materials 16 (6) (2023).
[16] A. Ahmad, et al., Aminocellulose - grafted polycaprolactone-coated core-shell nanoparticles alleviate the severity of ulcerative colitis: a novel adjuvant therapeutic approach, Biomater. Sci. 9 (17) (2021) 5868–5883.
[17] Y. Pu, et al., Harnessing polymer-derived drug delivery systems for combating inflammatory bowel disease, J. Contr. Release 354 (2023) 1–18.
[18] X. Fan, et al., An engineered butyrate-derived polymer nanoplatform as a mucosa-healing enhancer potentiates the therapeutic effect of magnolol in inflammatory bowel disease, ACS Nano 18 (1) (2024) 229–244.
[19] C. Jori, et al., Biomaterial-based strategies for immunomodulation in IBD: current and future scenarios, J. Mater. Chem. B 11 (25) (2023) 5668–5692.
[20] Z. Guo, et al., Thermosensitive polymer hydrogel as a physical shield on colonic mucosa for colitis treatment, J. Mater. Chem. B 9 (18) (2021) 3874–3884.
[21] M. Suhail, et al., Designing of pH-sensitive hydrogels for colon targeted drug delivery; characterization and in vitro evaluation, Gels 8 (3) (2022).
[22] I. Pulsoni, et al., Comparison between Franz diffusion cell and a novel micro-physiological system for in vitro penetration assay using different skin models, SLAS Technol 27 (3) (2022) 161–171.
[23] X. Wen, et al., Fecal microbiota transplantation alleviates experimental colitis through the Toll-like receptor 4 signaling pathway, World J. Gastroenterol. 29 (30) (2023) 4657–4670.
[24] N.H. Malibary, et al., Factors affecting ulcerative colitis flare-ups: associations with smoking habits and other patient characteristics, Cureus 13 (11) (2021) e19834.
[25] A. Croft, A. Lord, G. Radford-Smith, Markers of systemic inflammation in acute attacks of ulcerative colitis: what level of C-reactive protein constitutes severe colitis? J Crohns Colitis 16 (7) (2022) 1089–1096.
[26] J.V. Zanten, et al., Optimization of the production process of clinical-grade human salivary gland organoid-derived cell therapy for the treatment of radiation-induced xerostomia in head and neck cancer, Pharmaceutics 16 (3) (2024).
[27] E. Ban, et al., Poloxamer-Based thermoreversible gel for topical delivery of emodin: influence of P407 and P188 on solubility of emodin and its application in cellular activity screening, Molecules 22 (2) (2017).

[28] R.J. Porter, R. Kalla, G.T. Ho, Ulcerative colitis: recent advances in the understanding of disease pathogenesis, F1000Res 9 (2020).
[29] A.D. Rodgers, A.G. Cummins, CRP correlates with clinical score in ulcerative colitis but not in Crohn's disease, Dig. Dis. Sci. 52 (9) (2007) 2063–2068.
[30] T. Tian, Z. Wang, J. Zhang, Pathomechanisms of oxidative stress in inflammatory bowel disease and potential antioxidant therapies, Oxid. Med. Cell. Longev. 2017 (2017) 4535194.
[31] R. Banc, et al., Phytochemical profiling and biological activities of quercus sp. galls (oak galls): a systematic review of studies published in the last 5 years, Plants 12 (22) (2023).
[32] G. Kaur, et al., Antiinflammatory evaluation of alcoholic extract of galls of Quercus infectoria, J. Ethnopharmacol. 90 (2–3) (2004) 285–292.
[33] X. Han, et al., "Dual sensitive supramolecular curcumin nanoparticles" in "advanced yeast particles" mediate macrophage reprogramming, ROS scavenging and inflammation resolution for ulcerative colitis treatment, J Nanobiotechnology 21 (1) (2023) 321.
[34] B.S. Pabla, D.A. Schwartz, Assessing severity of disease in patients with ulcerative colitis, Gastroenterol Clin North Am 49 (4) (2020) 671–688.
[35] P. Rivière, et al., Deep ulcers are associated with increased C-reactive protein in active ulcerative colitis, Dig. Liver Dis. 55 (9) (2023) 1194–1200.
[36] Y.J. Liu, et al., Parthenolide ameliorates colon inflammation through regulating Treg/Th17 balance in a gut microbiota-dependent manner, Theranostics 10 (12) (2020) 5225–5241.
[37] O.C. Ulker, et al., Short overview on the relevance of microRNA-reactive oxygen species (ROS) interactions and lipid peroxidation for modulation of oxidative stress-mediated signalling pathways in cancer treatment, J. Pharm. Pharmacol. 74 (4) (2022) 503–515.
[38] Z. Wang, et al., Oxidative stress and liver cancer: etiology and therapeutic targets, Oxid. Med. Cell. Longev. 2016 (2016) 7891574.
[39] S.B. Chandraiah, et al., Substance P failed to reverse dextran sulfate sodium-induced murine colitis mediated by mitochondrial dysfunction: implications in ulcerative colitis, 3 Biotech 11 (4) (2021) 199.
[40] J.K. Yamamoto-Furusho, E.A. Mendieta-Escalante, Diagnostic utility of the neutrophil-platelet ratio as a novel marker of activity in patients with Ulcerative Colitis, PLoS One 15 (4) (2020) e0231988.
[41] G.E.O. Borgstahl, R.E. Oberley-Deegan, Superoxide dismutases (SODs) and SOD mimetics, Antioxidants 7 (11) (2018).
[42] A.Y. Baev, et al., Interaction of mitochondrial calcium and ROS in neurodegeneration, Cells 11 (4) (2022).